Spectrochimica Acta Part A: Molecular and Biomolecular Spectroscopy 176 (2017) 189–196

Contents lists available at ScienceDirect

Spectrochimica Acta Part A: Molecular and Biomolecular Spectroscopy

journal homepage: www.elsevier.com/locate/saa

Photo release of nitrous oxide from the hyponitrite ion studied by infrared spectroscopy. Evidence for the generation of a cobalt-N_2O complex. Experimental and DFT calculations

M. Elizabeth Chacón Villalba [a,b], Carlos A. Franca [a], Jorge A. Güida [a,c,d,*]

[a] CEQUINOR, Facultad de Ciencias Exactas, Universidad Nacional de La Plata, CONICET (CCT La Plata), Boulevard 120 N° 1465, 1900 La Plata, Argentina
[b] Comisión de Investigaciones Científicas CICPBA, Provincia de Buenos Aires, Argentina
[c] Departamento de Ciencias Básicas, Universidad Nacional de Luján, Luján, Argentina
[d] Departamento de Ciencias Básicas, Facultad de Ingeniería, Universidad Nacional de La Plata, La Plata, Argentina

ARTICLE INFO

Article history:
Received 6 September 2016
Received in revised form 27 December 2016
Accepted 2 January 2017
Available online 10 January 2017

Keywords:
Nitrous oxide complexes
Hyponitrite
Cobalt binuclear complex
Solid state photolysis
Infrared spectroscopy
Quantum chemical calculations
DFT

ABSTRACT

The solid state photolysis of sodium, silver and thallium hyponitrite ($M_2N_2O_2$, M = Na, Ag, Tl) salts and a binuclear complex of cobalt bridged by hyponitrite ($[Co(NH_3)_5\text{-}N(O)\text{-}NO\text{-}Co(NH_3)_5]^{4+}$) were studied by irradiation with visible and UV light in the electronic absorption region. The UV–visible spectra for free hyponitrite ion and binuclear complex of cobalt were interpreted in terms of Density Functional Theory calculations in order to explain photolysis behavior.

The photolysis of each compound depends selectively on the irradiation wavelength. Irradiation with 340–460 nm light and with the 488 nm laser line generates photolysis only in silver and thallium hyponitrite salts, while 253.7 nm light photolyzed all the studied compounds.

Infrared spectroscopy was used to follow the photolysis process and to identify the generated products. Remarkably, gaseous N_2O was detected after photolysis in the infrared spectra of sodium, silver, and thallium hyponitrite KBr pellets. The spectra for $[Co(NH_3)_5\text{-}N(O)\text{-}NO\text{-}Co(NH_3)_5]^{4+}$ suggest that one cobalt ion remains bonded to N_2O from which the generation of a $[(NH_3)_5CoNNO]^{+3}$ complex is inferred. Density Functional Theory (DFT) based calculations confirm the stability of this last complex and provide the theoretical data which are used in the interpretation of the electronic spectra of the hyponitrite ion and the cobalt binuclear complex and thus in the elucidation of their photolysis behavior.

Carbonate ion is also detected after photolysis in all studied compounds, presumably due to the reaction of atmospheric CO_2 with the microcrystal surface reaction products. Kinetic measurements for the photolysis of the binuclear complex suggest a first order law for the intensity decay of the hyponitrite IR bands and for the intensity increase in the N_2O generation. Predicted and experimental data are in very good agreement.

1. Introduction

Photochemistry of compounds related to NO and other biochemically and environmentally relevant nitrogen-oxygen species is of considerable current interest [1,2].

Hyponitrite ion, related structurally with NO, plays also a relevant biological role as intermediate species in the denitrification process in which the nitrous oxide is a product [3]. Specifically, the reduction of nitric oxide to nitrous oxide by NO reductase would be produced through a hyponitrite intermediary where the $N_2O_2^{2-}$ is bonded between two ferric iron centers [4,5].

The chemistry of the hyponitrite ion has been reviewed by Bonner et al. [6]. The hyponitrite ion and its conjugate acids are in equilibrium in aqueous solution; depending on the pH, all these species undergo decomposition [7]. In the photolysis of an aqueous suspension of silver hyponitrite, NO was generated as a consequence of light irradiation [8].

Nitrous oxide (N_2O) may be considered a derivative of the hyponitrite ion because the hyponitrous acid (HONNOH) decomposes in aqueous solutions (pH 4–14) into N_2O [7]. Nitrous oxide has been used in anesthetic practices for more than 150 years, and considered a major advance in anesthetics. However, the nitrous oxide administration is not without risk that may include hematologic, neurologic, myocardial, and immunologic effects [9].

* Corresponding author at: CEQUINOR, Facultad de Ciencias Exactas, Universidad Nacional de La Plata, CONICET (CCT La Plata), Boulevard 120 N° 1465, 1900 La Plata, Argentina.
E-mail address: guida@quimica.unlp.edu.ar (J.A. Güida).

http://dx.doi.org/10.1016/j.saa.2017.01.003
1386-1425/

The hyponitrous acid presents the trans (HON = NOH) configuration shown in Scheme 1a. Sodium hyponitrite show a cis [10] or trans [11] configuration, but in both cases the hyponitrite ion bonds *via* the oxygen (Scheme 1b). Cis and trans hyponitrites are geometrical isomers, with a rather large interconversion barrier (about 60 kcal/mol).

The hyponitrite ion may bond to a transition metallic centre in a number of ways. *cis*-Hyponitrite may coordinate a metal (Ni, Pt) through oxygen acting as a bidentate ligand in a pseudo-square configuration [12]. In a binuclear heme Fe—Cu complex the *trans*-hyponitrite ion bridges two metal centers coordinated by the nitrogen atom [13].

Nan Xu et al. [14] reported a binuclear iron porphyrin bridged by hyponitrite ion bonded by oxygen. In the binuclear cation studied in this work the hyponitrite bridge is coordinated in an asymmetric way (—N(O)NO—), being one cobalt nucleus bonded by oxygen and the other by nitrogen (see Scheme 1c) [15,16].

In the present work the sodium, silver and thallium hyponitrite salts and a binuclear complex of cobalt bridged by hyponitrite (μ-hyponitrite bis[pentaamminecobalt(III)]$^{4+}$) were studied by irradiation with light of different wavelengths. The compounds were photolyzed in the solid state to avoid the hyponitrite decomposition, possible side reactions and complex equilibria in aqueous solution. Quantum chemical calculations were also carried out to support experimental results.

2. Materials and Methods

2.1. Synthesis of the Studied Compounds

2.1.1. $[(NH_3)_5CoN(O)NOCo(NH_3)_5]^{4+}$ ($^{14/15}N$)

This cation was prepared with different anions (Br^-, NO_3^- and NO_3^- - Br^-) according to the method reported in reference 15.

2.1.2. $Ag_2N_2O_2$

1.5 ml of $AgNO_3$ 0.245 M was dropped under stirring on 3 ml of $Na_2N_2O_2$ 0.182 M. The yellow precipitate was separated by filtration and dried under P_2O_5 [11,17].

2.1.3. $Tl_2N_2O_2$

Stoichiometric amounts of $Na_2N_2O_2 \cdot H_2O$ and thallium sulphate were mixed in aqueous solutions (ice bath). The yellow precipitate was separated by filtration and dried under P_2O_5 [17].

2.1.4. $Na_2N_2O_2 \cdot H_2O$

Purchased from Sigma-Aldrich.

2.1.5. N_2O

Purchased from AGA Linde Healthcare.

2.2. Spectroscopic Measurements

The IR spectra of the substances as KBr pellets or Nujol mulls were recorded in the 4000 to 400 cm^{-1} range on a Bruker Equinox 55 FTIR spectrometer with 4 cm^{-1} resolution.

The UV–Visible spectra of the solutions were registered using Chrom Tech CT-5700 series spectrophotometer in the range of 190–1100 nm, with 2.0 nm resolution. Quartz cuvettes: 1 cm path length.

2.3. Light Sources and Irradiation Method

Ar^+ laser (488.0 nm line, 150 mW, 15 min); high pressure mercury lamp, (500 W, 340–460 nm, filtered with BG12 4 mm Schott, this includes mainly 365, 405 and 436 nm lines); low pressure mercury lamp Hanau, Germany (unfiltered) mainly 253.7 nm.

The initial (reference) infrared spectra of the samples were recorded before the irradiation process. After an irradiation period, the light source was turned off and the final infrared spectra of the samples, which were used in monitoring the photolysis process advances, were recorded.

In monitoring the photolysis, the infrared region 1200–900 cm^{-1}, which involves the hyponitrite bands and the infrared region around 2200 cm^{-1}, which involves the band due to (NN)N2O vibration, constituted the two target regions; the former to follow the reagent disappearance and the later to follow the products generation. It should be noted here that thallium and silver hyponitrite samples were darkened after irradiation, presumably by formation of respective oxides (M_2O, M = Tl, Ag, Na) (see Results and Discussion section).

2.4. Kinetic Measurements

Kinetic curves for binuclear complex of cobalt were calculated from band areas of infrared spectra scanned at different irradiation times (irradiation wavelength 253.7 nm). Experimental details for sample preparation and spectroscopic setup were described in Sections 2.2 and 2.3.

For the kinetics decay the hyponitrite band at 1033 cm^{-1} (δ(ONNO)) was chosen for area calculation because it shows the horizontal base line and it was not overlapping with other bands, and consequently, no extra band fit was required. For the products, increase the $\nu(NN)_{N2O}$ band at 2226 cm^{-1} was used because it is the most intense and is not overlapping. We use Opus software (version 4.2) of the Bruker infrared spectrometer for bands area calculation in the absorbance mode. The kinetic curves were then fitted by standard decay and rise functions discussed in Section 3.3.

2.5. Computational Details

Computational methods were used to investigate the electronic structure of the hyponitrite ion and the binuclear complex of cobalt.

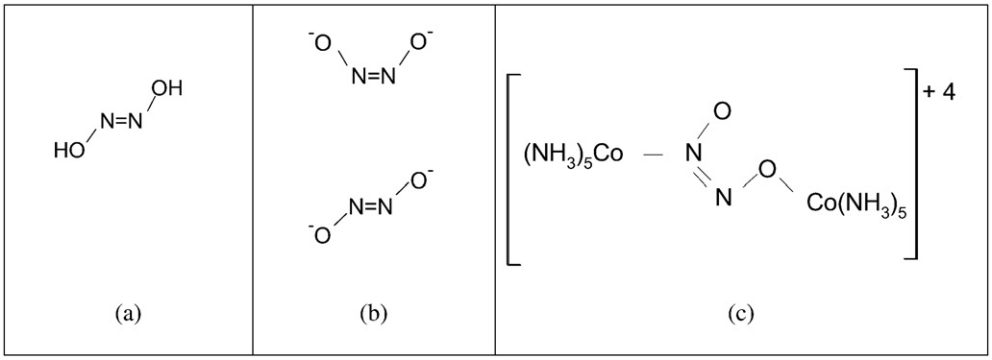

Scheme 1. Structure representation of hyponitrite moiety in different arrangements. (a) hyponitrous acid (b) sodium hyponitrite salts cis and trans (zig zag) (c) μ-N,O-hyponitrite bis[pentaamminecobalt (III)]$^{4+}$ cation ($[(NH_3)_5CoN(O)NOCo(NH_3)_5]^{4+}$).

Geometry optimization of both species was performed. The bulk solvation effect was considered by the approach of the conductor-like polarizable continuous model (CPCM) [18]. Absorption spectral properties were calculated by non-equilibrium time-dependent density functional theory (TDDFT) [19]. The simulated UV–visible based on Truhlar's functionals optimized geometries were calculated for the lowest 80 singlet-singlet electronic transitions. In these calculations, the Dunning-Huzinaga style augmented correlation-consistent-valance-polarized-triplezeta basis set (aug-cc-pVTZ) were used. For the hiponitrite anion [20,21], the calculations were performed with the M062X [24] hybrid DFT method [22]. The geometry optimization and frequency calculations performed for the binuclear complex, the M06-L hybrid DFT method [23] were preferred. The stabilities of the predicted six mononuclear cobalt complexes were tested by the DFT based calculations in order to support the photolysis reaction proposed here for the binuclear complex. The optimized geometry of $[(NH_3)_5CoNNO] + n$ and $[(NH_3)_5CoONN] + n$ ion complexes with $n = 2$ and $n = 3$ were calculated at M06-L/aug-cc-pVTZ level of theory by using Gaussian09 software [24]. The vibrational frequencies of these structures were also calculated at the same level of theory to confirm that they correspond to the local minima on the energy surfaces [25].

3. Results and Discussion

3.1. Electronic Spectra

The electronic spectrum of a silver hyponitrite suspension reported by Kumkely et al. [8], shows absorption bands at 207(sh), 255(sh) and 419 nm (wide). The last band was assigned to LMCT (Ligand Metal Charge Transfer).

Our electronic spectrum of solid thallium hyponitrite in KBr pellets shows absorption bands at 262, in the region 294–401 and 454 (sh) nm. In agreement with the wavelength reported by Poskrebyshev et al. ($\varepsilon(248\ nm) = 6550\ cm^{-1}\ M^{-1}$) [7], the electronic spectrum of sodium hyponitrite (see Fig. 1a) includes an absorption band at 246 nm, which is blue shifted with respect to silver and thallium hyponitrites.

The calculation performed with hybrid DFT methods provided a reliable interpretation of the observed electronic spectra of the hyponitrite ion and its photolysis behavior.

The experimental and calculated spectra of hyponitrite ion are compared in Fig. 1a. Theoretical calculations predict an absorption band at 238 nm (the envelope of the two main electronic transitions) in good agreement with the experimental data (*cf.* ref. 6). The assignments for electronic transitions predicted by quantum chemical calculations are collected in Table 1. The major contributions were found for the transitions at 272 and 233 nm. The first transition involves HOMO and LUMO + 3. The HOMO can be characterized as a π bonding molecular orbital mainly between the two atoms of nitrogen, and LUMO + 3 as π antibonding molecular orbitals mostly localized in N—O bonds (HOMO and LUMO + 3 are represented in Fig. 2). The transition at 233 nm, which involves HOMO–1 and LUMO + 2, was understood as a transition from a bonding orbital delocalized over all the atoms to a non-bonding orbital over the oxygen atoms.

The electronic spectra of the binuclear complex (aqueous solution) show bands at 212 nm ($\varepsilon \approx 6.9\ 10^5\ M^{-1}\ cm^{-1}$), 264 ($\varepsilon = 8.56\ 10^3\ M^{-1}\ cm^{-1}$), 302 (sh)nm ($\varepsilon = 5.33\ 10^3\ M^{-1}\ cm^{-1}$) and 484 nm ($\varepsilon = 227\ M^{-1}\ cm^{-1}$) (Fig. 1b). This spectrum was also interpreted with the aid of quantum chemical calculations. The assignments for the main electronic transitions predicted by DFT calculations are collected in Table 2. These are close to the experimental absorption bands.

The transition at 435 nm involves H-1 and L orbitals. H-1 can be described as a π non bonding orbital mainly located in the hyponitrite moiety and L as an orbital mainly centered in the O—Co—N bonding axis.

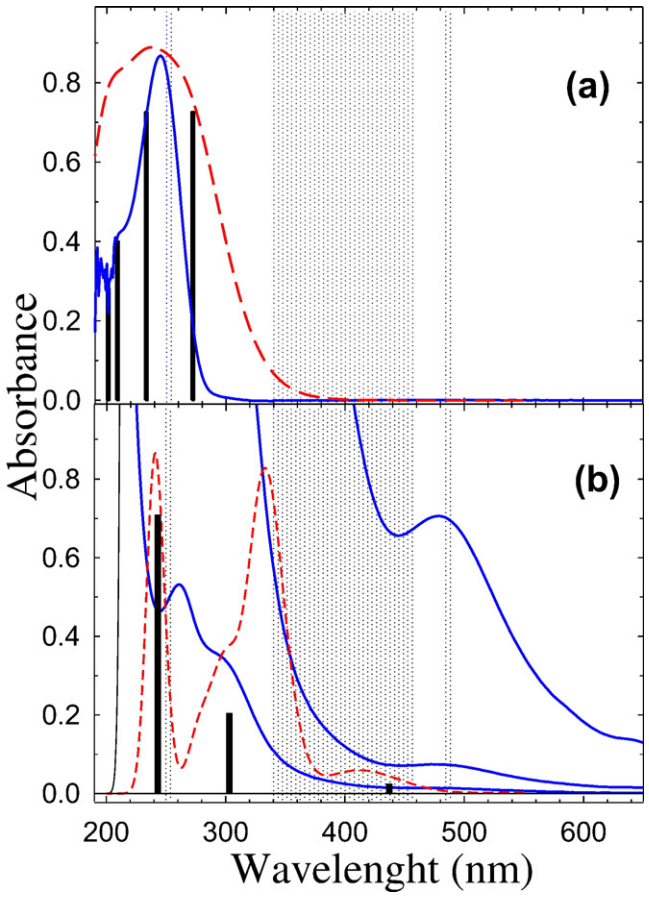

Fig. 1. (a) UV–visible spectra of $Na_2N_2O_2$ 2,4 10^{-4} M in aqueous solution at pH = 12 (blue line). Concentration value for $Na_2N_2O_2$ is only estimated due to contamination with sodium carbonate. Predicted spectra obtained from DFT theoretical calculations (dashed red). (b) UV–visible spectra of $[(NH_3)_5CoN(O)NOCo(NH_3)_5]^{4+}$ 3.10 10^{-3}, 3.10 10^{-4} and 6.21 10^{-5} M (blue) in aqueous solution. Predicted spectra obtained from calculations (dashed red). Vertical black bars in (a) and (b) specify predicted transitions (see Tables 1 and 2). Grey shadows show irradiation regions.

The transition at 301 nm involves the electron transfer from H-8 and H-2 to L, L + 1 and L + 3. H-8 and H-2 can be similarly described, showing contributions from hyponitrite N and O nonbonding orbitals, σ bonding (hyponitrite) and dxz-Co (O-bonded). L + 1 shows contributions from dx^2-y^2-Co (O-bonded) and L + 3 have contributions from π antibonding (hyponitrite) and dz^2 (both Co atoms).

The 241 nm transition involves the H (O—N nonbonding and N—N π bonding) and L + 4 (π antibonding hyponitrite) orbitals. Diagrams for the HOMO and LUMO + 4 molecular orbital of the binuclear complex of cobalt are depicted in Fig. 3.

The experimental and calculated spectra for $[(NH_3)_5CoN(O)NOCo(NH_3)_5]^{4+}$ ion are compared in Fig. 1b, where the irradiation zones which cover all the absorption regions are represented by shadows areas.

Table 1
Relevant predicted electronic transitions and their assignments for the free hyponitrite anion.

Wavelength (nm)	Osc. strength	Assignments
201	0.0704	H-2 → L + 1 (75%)
209	0.1000	H1 → L + 4 (90%)
233	0.1814	H1 → L + 2 (93%)
272	0.1815	HOMO → L + 3 (92%)

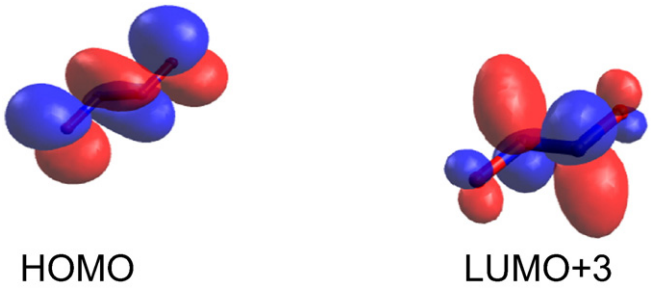

Fig. 2. The HOMO and LUMO + 3 of hyponitrite ion. An isovalue of 0.020 a.u. was used to construct the surfaces.

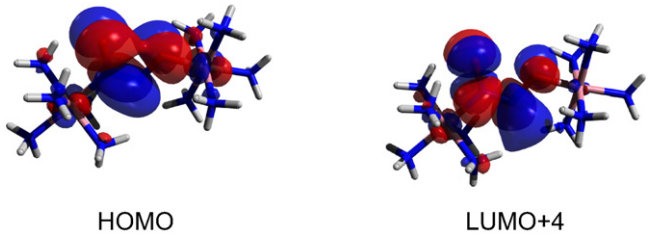

Fig. 3. The HOMO and LUMO + 4 of $[(NH_3)_5CoN(O)NOCo(NH_3)_5]^{4+}$ ion. An isovalue of 0.020 a.u. was used to construct the surfaces.

3.2. Hyponitrite Salts Photolysis

In order to monitor the photolysis progress, infrared spectra of pellets (samples dispersed in KBr matrix) were compared before and after irradiation, identifying the generated products. The electronic spectrum shown in Fig. 1S (Supplementary material) substantiate that the KBr is transparent to all radiation used in this work. Then, it is concluded that KBr could be used as a matrix component because it does not absorb any component of the employed radiation. The radiation sources were chosen so as to cover all the absorption regions in the electronic spectra of the samples.

The photolysis of hyponitrite salts is wavelength dependent, as it is inferred from the electronic spectra described above and for the irradiations results described below. While sodium hyponitrite undergoes photolysis only with the 253.7 nm line, thallium, and silver salts are photoinduced with all the wavelengths used in our irradiation set up. Moreover, darkening after irradiation was observed only in the silver and thallium hyponitrite pellets (see identification products below).

The electronic transitions theoretically predicted for the hyponitrite ion explain the observed electronic spectra of $Na_2N_2O_2$ (see Fig. 1a). It was assumed that both hyponitrite electronic transitions H-1 → L + 2 ($\pi \rightarrow \pi_{nb}$) and H → L + 3 ($\pi \rightarrow \pi^*$), predicted at 238 nm, may be induced by electronic excitation with light of 253.7 nm, very close to the experimental absorption band at 246 nm. However, this transition fails to reproduce the photolysis and the spectral shifts observed in thallium and silver hyponitrites. We then hypothesize that this is a possible (reversible) charge transfer transition proposed in the reference [8] from hyponitrite to metal that was not taken into account in the theoretical approach. On the other hand, the energy difference between HOMO hyponitrite and LUMO configurations for the Na^+, Tl^+ and Ag^+ ions in aqueous solution is expected in the sequence $\Delta E_{Na} > \Delta E_{Tl} > \Delta E_{Ag}$ in agreement with the experimental electronic spectral shifts.

Fig. 4 compares the infrared spectra of sodium, silver and thallium hyponitrites before and after irradiation with the 253.7 nm line. Characteristic ν(NO) bands (around 1000 cm^{-1}) decrease drastically with irradiation time and at the same time, a new feature around 2230 cm^{-1} appears after irradiation for each salt (Fig. 4). Since this new doublets at around 2230 cm^{-1} is very close and shows a very similar profile than that reported to ν(NN) of N_2O in the gaseous state [26] (see also Fig. 2S), we propose the formation of N_2O gas as a product of the photolysis of hyponitrite salts that remains caught in the solid state system. This was observed also in the binuclear complex as a singlet band at 2226 cm^{-1} (see following section).

Other bands grow during the irradiation of sodium hyponitrite salt at ~1400, 850, and 650 cm^{-1}. They are assigned to the asymmetric stretching (ν_3), out-of-plane bending $\pi(CO_3)$ (ν_2) and δ(OCO) (ν_4), respectively, corresponding to a carbonate ion generated during the photolysis [27].

Fig. 5 shows the overall picture of the sodium hyponitrite infrared spectra before and after irradiation and the sodium carbonate reference. The $\nu(CO)_{as}$ was also found in the infrared spectra of the irradiated binuclear complex as a widening of the 1391 cm^{-1} band ($\nu(NN)_{N2O2}$).

To show whether the samples undergoes photolysis without atmospheric CO_2, hyponitrite salts were irradiated under vacuum. For such purpose a quartz tube connected to a gas cell fitted with KBr windows were assembled (see Fig. 3S Supplementary material). Pure samples of sodium, thallium and silver hyponitrites (without KBr dilution) were irradiated into the quartz tube under vacuum with UV light (253.7 nm). The infrared spectrum of the gas cell scanned after irradiation of a sodium hyponitrite is shown in Fig. 2S. This spectrum is compared in the

Table 2
Relevant electronic transitions predicted for $[(NH_3)_5CoN(O)NOCo(NH_3)_5]^{4+}$ and their assignments.

Wavelength(nm)	Osc. strength	Assignment
241	0.236	H → L + 4 (69%)
301	0.068	H-8 → L + 1 (20%)
		H-8 → L + 3 (16%)
		H-2 → L + 3 (20%)
		H-2 → L (17%)
435	0.008	H-1 → L (74%)

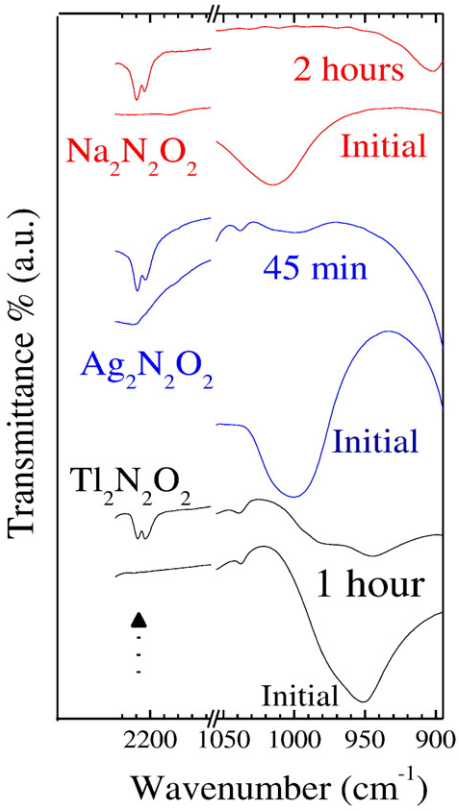

Fig. 4. Infrared spectra of hyponitrite salts (sodium, silver and thallium) before and after irradiation with 253.7 nm light. For better viewing the spectra have been displaced vertically relative to each other. The arrow points to the N_2O (*doublet*) product reaction.

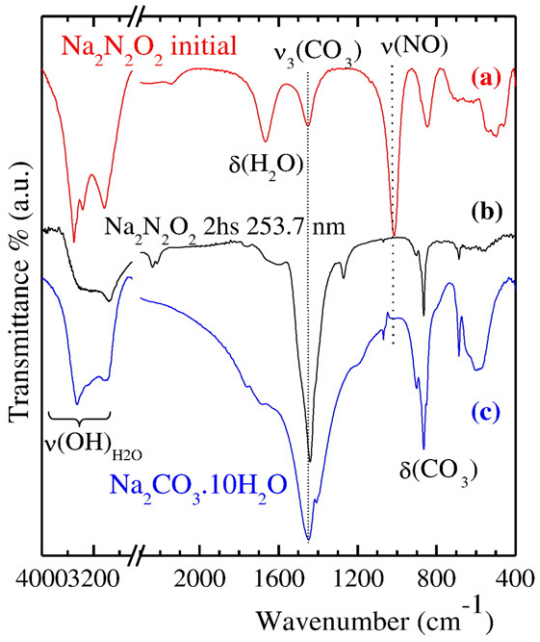

Fig. 5. Infrared spectra of $Na_2N_2O_2$ before (a) and after (b) irradiation ($\lambda = 253.7$ nm) and the comparison with sodium carbonate spectra (c).

same figure with that coming from a N_2O cylinder in the same instrument under similar conditions. Since both spectra are identical it is concluded that the N_2O is also generated without the presence of atmospheric CO_2 and confirms that the reaction proceeds even without potassium bromide. We then suggest that the atmospheric CO_2 freely penetrates the pellet samples, but why the N_2O does not escape from the solid? The suggestion that the CO_2 freely penetrates the samples and the N_2O is being unable to escape from it, are mutually exclusive. The last statement and the darkness observed in silver and thallium hyponitrites samples require further explanation. The CO_2 penetration and N_2O entrapment could be compatible under the assumption that the N_2O is trapped in the hyponitrite packing while the CO_2 penetrates the KBr pellets and reacts with the products of reaction on the microcrystal surface. Due to photolysis, the formation of M_2O (M = Tl, Na, Ag) inside the microcrystal arises as a necessary product. It is also compatible with the darkness observed in silver and thallium hyponitrites after photolysis.

To check if silver remains in the oxidation state I after $Ag_2N_2O_2$ photolysis, the chemical reaction proposed in [8] was tested. It was noted that the black solid contacted with ammonia solution (50%) dissolved immediately at room temperature. Since elemental silver does not dissolve in aqueous ammonia, it was inferred that silver remains in oxidation state I (Ag_2O) after photolysis.

The products of photolysis identified in this work are not in agreement with those reported in [8] for the irradiation of silver hyponitrite. In fact, in that work the reported products of irradiation were elemental silver and nitric oxide and this conclusion was indirectly inferred from subsequent reactions of nitric oxide with oxygen and water to produce nitrous acid, which was detected in electronic spectra [8]. Therefore, the difference between those results and the present results are due probably to Kumkely et al. carrying out their measurements in an aqueous suspension. It seems therefore that infrared spectroscopy is a better analytical tool to determine products after photolysis in the solid state instead of indirect methods.

3.3. Binuclear Complex Photolysis

To analyze the changes during the irradiation we first review briefly the known infrared spectra of the binuclear complex. The infrared spectra of binuclear cobalt hyponitrite show a distinctive band pattern than that of sodium, thallium and silver hyponitrites, as expected from bond description shown in Scheme 1 (Table 3).

Mercer et al. [28] and Miki and Ishimori [29] reported the infrared spectrum of the binuclear complex cation. For a better assignment, these two studies included infrared spectra after ^{15}N bridge substitution (50%). More recently, a structural study and reinterpretation of the vibrational spectra of the binuclear complex was published [15]. This included the first Raman spectra allowing new assignments for the bridged —ONN(O)— moiety. The information provided was also supported by quantum chemical calculations. The ν(NN) band was individualized when the nitrate counterions were replaced by bromide ions avoiding the overlap of nitrate anti-symmetrical stretching mode (ν_3(NO)) to the $\nu(NN)_{hyponitrite}$ band at 1391 cm^{-1}. Infrared wavenumbers for hyponitrite ions in the cobalt binuclear complex (^{14}N, ^{15}N) [15,28,29] and sodium [27,30,31], silver and thallium hyponitrite salts (this work) are summarized in Table 3.

Wavenumbers for the binuclear complex were also calculated in this work using a more precise quantum method than that reported in Ref. [15]. The values obtained for the hyponitrite moiety were then collected in Table 1S (Supplementary material) and compared with the experimental and theoretical values reported in [15]. It can be seen from this table that the frequencies of hyponitrite modes are confirmed and that the values in the present work are closer to the experimental than those reported [15].

The KBr-binuclear complex pellets were sequentially irradiated with the 488.0 nm (Ar^+ laser), 340–460 nm (from high pressure mercury lamp filtered) and 253.7 nm (from low pressure mercury lamp) lines. As mentioned above for the hyponitrite salts, photolysis progress was monitored scanning infrared spectra before and after each irradiation. The light selected for irradiation cover all absorption regions of the studied compound. We observed that the binuclear complex photolysis only progressed when the wavelength of exciting radiation was 253.7 nm. This wavelength is close to the absorption band at 264 nm and to the predicted transition by quantum chemical calculations at 241 nm. This was understood as a transition from O—N nonbonding and N—N π bonding to π antibonding hyponitrite (intraligand charge transfer). We hypothesize that the bond order reduction produced in hyponitrite moiety by the electronic transition may induce the chemical reaction observed experimentally.

Interestingly, the electronic transition that generate photolysis in sodium hyponitrite have the same description predicted for the binuclear complex of cobalt, although the molecular geometry and hyponitrite bonds are different. Moreover, photolysis in both compounds is caused by the same irradiation wavelength and shows similar magnitude for the molar extinction coefficient (ε). A better comparison should consider lattice effects.

The characteristic infrared bands of bridged hyponitrite in the Co-binuclear complex were located in the spectral region 1400–900 cm^{-1}. Fig. 6 shows a selected infrared spectral region of the binuclear complex (KBr pellet) before and after irradiation with light of 253.7 nm. This figure also shows the spectra of a sample containing the ^{15}N labelled-bridge. It can be seen that hyponitrite bands decrease with increasing time of irradiation whereas a new band grows at

Table 3
Infrared bands (cm^{-1}) observed for $N_2O_2^{2-}$ moiety in $[(NH_3)_5CoN(O)NOCo(NH_3)_5]Br_4$ (^{14}N, ^{15}N) and hyponitrite salts (sodium, silver and thallium).

Assignments	$N_2O_2^{2-}$ binuclear complex			$N_2O_2^{2-}$ (anion)		
	^{14}N	^{15}N	Shifts	Na	Ag	Tl
ν(NN)	1391 m	1348	43			
ν(NO)	1124 m	1096	28	1013	998	941
δ(ONNO)	1033 m	1013	20			
ν(NO)	917 m	905	11			
δ(ONNO)	600 vw					

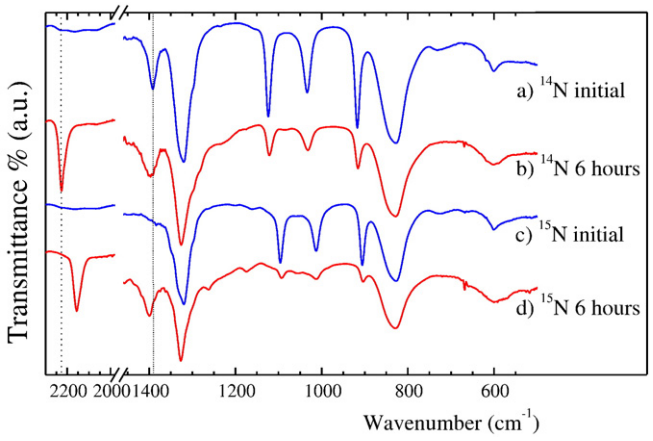

Fig. 6. Infrared spectra of $[(NH_3)_5CoN(O)NOCo(NH_3)_5]Br_4$ (KBr pellet) before and after irradiation ($\lambda = 253.7$ nm). For a better view, the spectra have been displaced vertically with respect to each other. a. Normal sample before irradiation; b. After 6 h of irradiation; c. Sample containing the hyponitrite bridge ^{15}N labelled before irradiation; f. Sample ^{15}N labelled after 6 h of irradiation. The arrow points to the N_2O (*singlet*) product reaction.

2226 cm^{-1} for the normal sample and at 2157 cm^{-1} for the ^{15}N substituted-sample. Besides, a new shoulder at 1282 cm^{-1} and band broadening at 588 cm^{-1} are detected. These features were confirmed by difference spectra. For the ^{15}N labelled sample these bands are shifted to 1261 and 580 cm^{-1}, respectively. The wavenumbers and the relative infrared intensities in this study for the two set of bands (^{14}N and ^{15}N) are in agreement with those previously reported for N_2O gas [26,30,31]. Accordingly, we propose to assign the infrared bands observed at 2226, 1282 and 588 cm^{-1} as well as those observed at 2157, 1261 and 580 cm^{-1} to the ν(NN), ν(NO) and δ(NNO) vibrations of N_2O for the ^{14}N and the ^{15}N substituted samples [31], respectively.

The ν(NN) band at around 1391 cm^{-1} (^{14}N normal samples) of the hyponitrite bridge becomes wider after irradiation. For the ^{15}N substituted sample (Fig. 6d) it is shifted to 1348 cm^{-1} as a shoulder of a very strong band at 1321 cm^{-1} (δ(NH_3)) [15]. In spite of this shift, in the isotopic ^{15}N sample, the band at 1399 cm^{-1} still grows after irradiation. It is concluded, therefore, that this new band is not related to the bridge decomposition because it does not move its spectral position with ^{15}N isotopic substitution. We reason that this may be due to carbonate ion formation in the reaction between photolysis products with atmospheric CO_2.

The photolysis process was not completed after 6 h of irradiation, as shown by the features associated to the hyponitrite bridge which did not vanish entirely. To verify whether the carbonate bands come from atmospheric CO_2, two additional photolysis were carried out: one irradiation with the sample under vacuum (Oxford cryostat (OX8ITL) with KBr optical windows) and other with KBr pellets soaked with halocarbon oil. We find that in both set ups the photolysis progressed following the same behavior as hyponitrite salts under vacuum, but, on the other hand, carbonate bands (1400, 850, and 650 cm^{-1}) were not observed after photolysis. Then, we concluded that the measured carbonate bands came from the atmospheric CO_2.

We review in Table 4 N_2O infrared bands under different conditions in order to explain why after photolysis the $\nu(NN)_{N2O}$ is observed as doublet in hyponitrite salts and as a singlet in the binuclear complex. While some of these were taken from our spectra others associated with different compounds, including N_2O moiety, were from the current literature.

This includes the unusual ruthenium and osmium N_2O complexes [32,33] and low temperature matrices of N_2O diluted in argon, xenon [34] and nitrogen [31]. Accordingly, a singlet ν(NN) would be expected either if the N_2O molecule bonds to a transition metal forming a complex or if it is trapped in a matrix at low temperature. In both cases no vibro-rotational contour would be observed because molecular rotations are inhibited (a typical doublet is observed for a free linear molecule). Therefore, the singlet band formed at 2226 cm^{-1} during the irradiation of the binuclear complex should be attributed to the N_2O moiety coordinated with one cobalt center.

Table 4
Nitrous oxide wavenumbers in gas phase, matrix, complexes and photolysis products for different hyponitrites.

Compound	ν(NN)	ν(NO)	δ(NNO)	Reference
Gas N_2O	2234/2216	1301 1274	589	This work
$Na_2N_2O_2$	2239/2216			This work
$Tl_2N_2O_2$	2237/2217			This work
$Ag_2N_2O_2$	2238/2216			This work
$Co[NN]Br_4$[a]	2226	1282 (sh)	588	This work
$Co[^{15}N^{15}N]Br_4$[a]	2157	1261	580	This work
N_2O in N_2 matrix (15 K)	2236	1291	589	[31]
$^{15}N_2O$ in N_2 matrix (15 K)	2166	1272	573	[31]
$[Ru(NH_3)_5N_2O]^{2+}$[b]	2234 (2234 calc)	1150 (1150calc)	298 (296calc)	[32]
$[Ru(NH_3)_5\ ^{15}N_2O]^{2+}$[b]	2209 (2209 calc)	1137 (1136calc)	296 (296calc)	[32]
$[Os(bpy)Cl_3N_2O]^{1-}$[c]	2252	1245	536/533	[33]
N_2O in Xe matrix	2215	1280	584	[34]
N_2O in Ar matrix	2219	1283	589	[34]
N_2O adsorbed in ZnO	2237	1650–1200	–	[35]

[a] Photolized ($Co[NN]Br_4$: $[(NH_3)_5CoN(O)NOCo(NH_3)_5]Br_4$).
[b] Isolated.
[c] It should be noted that according to Laane [31] and Paulat [32] the assignment of bands ν(NN) and ν(NO) in $[Os(bpy)Cl_3N_2O]$ [33], may be reversed.

This assumption is supported by the fact that the Ag, Tl, Na cations do not produce any complex with the N_2O, and the observed doublet does not shift significantly from the N_2O(g) band positions, suggesting weak interaction between them (see arrow in Fig. 6). Hussain et al. reported a single band at 2237 cm^{-1} when N_2O is co-adsorbed on ZnO at room temperature [35]. This observed singlet band suggests a strong interaction (or a chemical bond) between N2O and Zn2 + which can be compared to that determined for the binuclear complex studied in this work.

A single $\nu(NN)_{N2O}$ band has also been reported for the $[Ru(NH_3)_5N_2O]^{2+}$ [32] and $[Os(bpy)Cl_3N_2O]^{1-}$ complexes [33], in which the N_2O moiety binds to Ru(II) and Os(II) ions.

The single band observed for the $\nu(NN)_{N2O}$ mode after the photolysis of cobalt-binuclear complex suggests a bond between Co and N_2O.

The stability of the possible $[(NH_3)_5CoN_2O]^{+n}$ complex was tested by DFT calculations in order to support our conclusions on reaction products proposed for the binuclear complex. The optimizations for the six possible configurations for the $[(NH_3)_5CoNNO]^{+n}$ and $[(NH_3)_5CoONN]^{+n}$ ions, with $n = 2$ and $n = 3$ were carried out with M06-L density functional and TZVP basis sets. For $n = 2$ low and high spins configurations were considered. Only two of the six likely complex structures converged to a minimum in the potential energy surface; these are $[(NH_3)_5CoNNO]^{+3}$ and $[(NH_3)_5CoONN]^{+3}$. The energy of the first is 7.63 Kcal/mol lower than the second, supporting the idea that a $[(NH_3)_5CoNNO]^{+3}$ species could be produced after photolysis of the binuclear complex of cobalt.

The wavenumbers for $[(NH_3)_5CoNNO]^{3+}$ and $[(NH_3)_5CoONN]^{3+}$ hypothetical structures were calculated. In Table 2S (Supplementary materials) the calculated frequency for the —NNO moieties in both arrangements are compared with observed values. This table shows that the linkage isomer Co—ONN vibrational frequencies are closer to the experimental values than those of Co—NNO. However, the wavenumber agreement is not so good to allow discarding beforehand neither of the two configurations.

Based on the above results, the following reactions are therefore proposed for the hyponitrite salts photolysis. Inside the microcrystals:

$$2\ M_2N_2O_2 \xrightarrow{h\nu} 2\ N_2O(g)\ \text{(trapped)} + M_2O \quad (M = Na, Tl, Ag)$$

The photo-reactions are not reversible and the $N_2O(g)$ trapped in the corresponding microcrystals could be detected in the IR spectra.

The reaction with carbon dioxide is proposed for the microcrystal surface. The $N_2O(g)$ generated on the surface would not be trapped in the KBr matrix and then:

$$M_2N_2O_2 + CO_2(g) \xrightarrow{h\nu} M_2CO_3 + N_2O(g)\uparrow$$

A similar result is observed for the binuclear complex, although in this case the formed N_2O possibly remains bound to Co. Like in the previous case of saline hyponitrites, the carbonate bands were also detected when the photolysis of the binuclear complex proceeds under atmospheric CO_2. Based on the results discussed above, the following products are proposed inside the microcrystals:

$$\left[(NH_3)_5Co{-}N(O) = N{-}O{-}Co(NH_3)_5\right]^{4+} \xrightarrow{h\nu} \left[(NH_3)_5CoNNO\right]^{3+} + \left[(NH_3)_5CoO\right]^{+1}$$

The products of reaction may react with atmospheric CO_2 according to:

$$\left[(NH_3)_5Co{-}N(O) = N{-}O{-}Co(NH_3)_5\right]^{4+} + CO_2 \xrightarrow{h\nu} \left[(NH_3)_5CoNNO\right]^{3+} + \left[(NH_3)_5CoCO_3\right]^{+1}$$

The degree of interaction of N_2O with transition metals may be discussed comparing bands position in different complexes. It is found that ν(NN) bands move to higher frequencies in complexes of Co, Ru, Os while ν(NO) shifts to lower ones (Table 2), whereas no correlation for the δ(NNO) bands could be determined from the available data. These results suggest that the N_2O interaction with metal increases in the order Co < Ru < Os.

The kinetics of the binuclear complex photolysis was also followed by infrared spectroscopy. Fig. 7 shows the decrease of the δ(ONNO) band area at 1033 cm^{-1} (red triangles) and the simultaneous increase of the $\nu(NN)_{N2O}$ band area at 2226 cm^{-1} (blue circles). Band area for both are shown in Table 3S (Supplementary materials). For the first mode, the decay of the band area was fitted using the exponential decay function $y = y_0 + a\ e^{-kt}$ with $a = 1.93 \pm 0.08\ cm^{-1}$ and $k = 0.022 \pm 0.003\ min^{-1}$, which shows that the decay area of bridge bands follows a first order law.

The growth of the $\nu(NN)_{N2O}$ band area mode was fitted using the function $y = a(1 - e^{-kt})$ with: $a = 3.44 \pm 0.02$ and $k = 0.0237 \pm 0.0006\ min^{-1}$. Since both fitting functions yield the same k values we conclude that N_2O is generated from the decay of the bridge. Fig. 7 shows a good agreement between the kinetic experimental values (circles) and the fitting functions (black lines). Fitness details for the decay and raise functions were detailed in Supplementary Material.

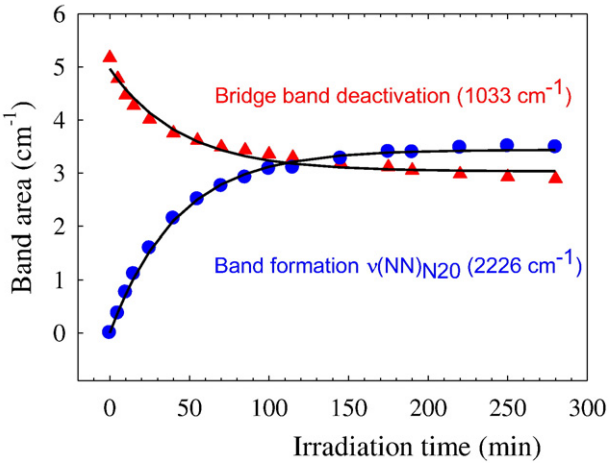

Fig. 7. Kinetic photolysis for $[(NH_3)_5CoN(O)NOCo(NH_3)_5](NO_3)_2Br_2$. (▲): Experimental band area for $\delta(ONNO)_{bridge}$ mode (1033 cm^{-1}) and (●): Experimental band area for $\nu(NN)_{N2O}$ mode (2226 cm^{-1}). Predicted curves for first order law are depicted in black lines (see text).

4. Conclusions

In this work the photolysis behavior of sodium, silver, and thallium salts of the hyponitrite anion as well as of a binuclear complex of cobalt bridged by the hyponitrite anion, were investigated. In all cases the samples were irradiated in the solid state with different wavelengths, in coincidence with the absorption region of each electronic spectrum.

It was found that the photolysis of each compound depends selectively on the irradiation wavelength. Irradiation with 340–460 nm light and with the 488 nm laser line generates photolysis only in silver and thallium hyponitrite salts, while 253.7 nm light photolyzed all the studied compounds.

DFT calculations explained the electronic spectra of the free hyponitrite ion and of the binuclear complex of cobalt in aqueous solution because predicted transitions are close to the absorption band peaks. Successful photolysis, achieved in all compounds with light of 253.7 nm, may also be assigned by DFT calculations. A charge transfer transition inside the hyponitrite moiety from π bonding molecular orbitals to π antibonding $N_2O_2^{2-}$, either in the free hyponitrite ion and in the binuclear complex may induce the reaction observed in all samples. However, calculations are unable to account for the photolysis in the sodium, thallium, and silver hyponitrite salts. We assume that an additional reversible charge transfer transition from hyponitrite to the metal might induce the photolysis processes for silver and thallium hyponitrites which produce the pellets darkening as consequence of M_2O formation.

The products of photolysis were detected by infrared spectroscopy. N_2O bands are observed for all the compounds after photolysis. Carbonate bands were also detected after photolysis when the samples are exposed to air. The photolysis at the solid state favored the identification of products by infrared spectroscopy which cannot be carried out in solution.

The generation of nitrous oxide by the photolysis in our compounds, in the solid state, is unambiguously determined. However, the spectral profile of nitrous oxide obtained in the hyponitrite salts is different than that observed for the binuclear complex. For the first case, the observed bands are due to free N_2O molecules trapped in the microcrystals, while for the second, the observed single band is due to bonded N_2O groups, similar to that measured for the nitrous oxide complexes reported in the literature [32,33].

Therefore, we conclude that these are the evidences for the formation of a cobalt complex with nitrous oxide, which results from irradiation of the binuclear complex.

The proposed formation and stability of a $[(NH_3)_5Co(N_2O)]^{+3}$ complex is supported by DFT calculations.

It should be remarked here that different structures of hyponitrite ions were irradiated in this work (see comparison in Scheme 1b (down) with 1c), however, the common product generated in all the photolysis process is N_2O molecule.

Kinetic measurements for binuclear complex photolysis may be explained by a first order law either for the intensity decay of hyponitrite IR bands or for the intensity increase due to N_2O generation. Kinetic parameters also suggest that the N_2O generation is originated in the hyponitrite bridge decomposition.

Acknowledgements

This work was supported by the following institutions: Consejo Nacional de Investigaciones Científicas y Técnicas (CONICET, grants: PIP 5633/05 and 0327), Agencia Nacional de Promoción Científica y Tecnológica (Grants PICT 06-11127 and 1539, PME 2006-00069-05), Facultad de Ciencias Exactas, Universidad Nacional de La Plata (14/B15), and Universidad de Luján (11/X565 and 11/X672), República Argentina. J.A.G. also thanks to PROMEI Program, Facultad de Ingeniería, UNLP for the UV–Visible spectrophotometer. CAF acknowledges the Universidad Nacional de Catamarca for computing time.

M. E. Ch. V. is member of Professional Staff of Comisión de Investigaciones Científicas, Provincia de Buenos Aires, Argentina (CICPBA). J. A. G. is member of Research Staff of Consejo Nacional de Investigaciones Científicas y Técnicas (CONICET) and Associate Professor at Facultad de Ingeniería, UNLP, Argentina. The authors also thank Ing. C. Young, N.E. Massa and E.L. Varetti for their suggestions and careful correction to the manuscript.

Appendix A. Supplementary data

Supplementary data to this article can be found online at http://dx.doi.org/10.1016/j.saa.2017.01.003.

References

[1] P.C. Ford, Photochemical delivery of nitric oxide, Nitric Oxide 34 (2013) 56–64.
[2] M.J. Rose, P.K. Mascharak, Fiat lux: selective delivery of high flux of nitric oxide (NO) to biological targets using photoactive metal nitrosyls, Curr. Opin. Chem. Biol. 12 (2008) 238–244.
[3] W.C. Troggler, Physical properties and mechanisms formation of nitrous oxide, Coord. Chem. Rev. 187 (1999) 303–327.
[4] T.C. Berto, N. Xu, S.R. Lee, A.J. McNeil, E.E. Alp, J. Zhao, G.B. Richter-Addo, N. Lehnert, Characterization of the bridged hyponitrite complex {[Fe(OEP)]$_2$(μ-N_2O_2)}: reactivity of hyponitrite complexes and biological relevance, Inorg. Chem. 53 (2014) 6398–6414.
[5] S. Chakraborty, J. Reed, J.T. Sage, N.C. Branagan, I.D. Petrik, K.D. Miner, M.Y. Hu, J. Zhao, E.E. Alp, Y. Lu, Recent advances in biosynthetic modeling of nitric oxide reductases and insights gained from nuclear resonance vibrational and other spectroscopic studies, Inorg. Chem. 54 (2015) 9317–9329.
[6] F.T. Bonner, M.N. Hughes, The aqueous solution chemistry of nitrogen in low positive oxidation states, Comments Inorg. Chem. 7 (1988) 215–234.
[7] G.A. Poskrebyshev, V. Shafirovich, S.V. Lymar, Hyponitrite radical, a stable adduct of nitric oxide and nitroxyl, J. Am. Chem. Soc. 126 (2004) 891–899.
[8] H. Kumkely, A. Vogler, Generation of nitric oxide by photolysis of silver hyponitrite. in suspension induced by LMCT excitation, Inorg. Chem. Commun. 10 (2007) 1294–1296.
[9] R.D. Sanders, J. Weimann, M. Maze, Biologic effects of nitrous oxide, Anesthesiology 109 (2008) 707–722.
[10] C. Feldmann, M. Jansen, *cis*-Sodium hyponitrite-a new preparative route and a crystal structure analysis, Angew. Chem. Int. Ed. 35 (1996) 1728–1730.
[11] N. Arulsamy, D. Scott Bohle, J.A. Imonigie, E.S. Sagan, Synthesis and characterization of alkylammonium hyponitrites and base-stabilized hyponitrous acid salts, Inorg. Chem. 38 (1999) 2716–2725.
[12] a) N. Arulsamy, D. Scott Bohle, J.A. Imonigie, S. Levine, An Umpolung approach to cis-hyponitrite complexes, Angew. Chem. Int. Ed. 41 (2002) 2371–2373;
b) N. Arulsamy, D. Scott Bohle, J.A. Imonigie, R.C. Moore, Group 8 and 10 hyponitrite and dinitrosyl complexes, Polyhedron 26 (2007) 4737–4745.
[13] C. Varotsis, T. Ohta, T. Kitagawa, T. Soulimane, E. Pinakoulaki, The structure of the hyponitrite species in a heme Fe - Cu binuclear center, Angew. Chem. Int. Ed. 46 (2007) 2210–2213.
[14] a) A. Nan Xu, L.O. Campbell, D.L. Powell, J. Khandogin, G.B. Richter Addo, A stable hyponitrite-bridged iron porphyrin complex, J. Am. Chem. Soc. 131 (2009) 2460–2461;
b) J.Y. Nan Xu, G.B. Richter Addo, Linkage isomerization in heme-NOx compounds: understanding NO, nitrite, and hyponitrite interactions with iron porphyrins, Inorg. Chem. 49 (2010) 6253–6266.
[15] M.E. Chacón Villalba, J.A. Güida, E.L. Varetti, P.J. Aymonino, New structural study and reinterpretation of the vibrational spectra of the l-N,O-hyponitrite bis[pentaamminecobalt(III)]4+ cation, Inorg. Chim. Acta 359 (2006) 707–712.
[16] B.F. Hoskins, F.D. Whillans, Crystal and molecular structure of a μ-hyponitrito-*bis*[penta-ammine-cobalt(III)] salt: the nature of the red nytrosylpenta-amminecobalt(III) cation, J. Chem. Soc. Dalton (1973) 607–611.
[17] G. Brauer, Quimica Inorgánica Preparativa. Ed. Reverté Barcelona, 1958 (306 pp).
[18] T.H. Dunning Jr., Gaussian basis sets for use in correlated molecular calculations. I. The atoms boron through neon and hydrogen, J. Chem. Phys. 90 (1989) 1007–1023.
[19] (a) M.E. Casida, C. Jamoroski, K.C. Casida, D.R. Salahub, J. Chem. Phys. 108 (1998) 4439–4449;
(b) R.E. Stratmann, G.E. Scuseria, M.J. Frisch, J. Chem. Phys. 109 (1998) 8218–8224;
(c) R. Bauernschmitt, R. Ahlrichs, Chem. Phys. Lett. 256 (1996) 454–464.
[20] R.A. Kendall, T.H. Dunning Jr., R.J. Harrison, Electron affinities of the first-row atoms revisited. Systematic basis sets and wave functions, J. Chem. Phys. 96 (1992) 6796–6806.
[21] P. Hohenberg, W. Kohn, Inhomogeneous electron gas, Phys. Rev. 136B (1964) 864–871.
[22] R.G. Parr, W. Yang, Density Functional Theory of Atoms and Molecules, Oxford University Press, 1989 (333 pp).
[23] Y. Zhao, D. Truhlar, Acc. Chem. Res. 41 (2) (2008) 157.
[24] M.J. Frisch, G.W. Trucks, H.B. Schlegel, G.E. Scuseria, M.A. Robb, J.R. Cheeseman, G. Scalmani, V. Barone, B. Mennucci, G.A. Petersson, H. Nakatsuji, M. Caricato, X. Li, H.P. Hratchian, A.F. Izmaylov, J. Bloino, G. Zheng, J.L. Sonnenberg, M. Hada, M. Ehara, K. Toyota, R. Fukuda, J. Hasegawa, M. Ishida, T. Nakajima, Y. Honda, O. Kitao, H. Nakai, T. Vreven, J.A. Montgomery Jr., J.E. Peralta, F. Ogliaro, M. Bearpark, J.J. Heyd, E. Brothers, K.N. Kudin, V.N. Staroverov, T. Keith, R. Kobayashi, J. Normand, K. Raghavachari, A. Rendell, J.C. Burant, S.S. Iyengar, J. Tomasi, M. Cossi, N. Rega, J.M. Millam, M. Klene, J.E. Knox, J.B. Cross, V. Bakken, C. Adamo, J. Jaramillo, R. Gomperts, R.E. Stratmann, O. Yazyev, A.J. Austin, R. Cammi, C. Pomelli, J.W. Ochterski, R.L. Martin, K. Morokuma, V.G. Zakrzewski, G.A. Voth, P. Salvador, J.J. Dannenberg, S. Dapprich, A.D. Daniels, O. Farkas, J.B. Foresman, J.V. Ortiz, J. Cioslowski, D.J. Fox, Gaussian 09, Revision B.01, Gaussian Inc., Wallingford CT, 2010.
[25] F. Weigend, R. Ahlrichs, Balanced basis sets of split valence, triple zeta valence and quadruple zeta valence quality for H to Rn: design and assessment of accuracy, Phys. Chem. Chem. Phys. 7 (2005) 3297–3305.
[26] The Sadtler Standard Spectra, GS135, Sadtler Research Laboratories, Philadelphia, PA 19104, USA, 1972.
[27] G.E. McGraw, D.L. Bernitt, I.C. Hisatsune, Infrared spectra of isotopic hyponitrite ions, Spectrochim. Acta 23A (1967) 25–34.
[28] E.E. Mercer, W.A. McAllister, J.B. Durig, An Infrared and Chemical Investigation of the two isomers of the pentaamminenitrosylcobalt ion, Inorg. Chem. 6 (1967) 1816–1821.
[29] E. Miki, T. Ishimori, New red pentaamminenitrosylcobalt(III) complexes obtained by the reaction of a cobalt (II)-ammoniacal solution with nitrogen oxide, Bull. Chem. Soc. Jpn. 49 (1976) 987–993.
[30] K. Nakamoto, Infrared and Raman Spectra of Inorganic and Coordination Compounds, sixth ed. Wiley, New Jersey USA, 2009.
[31] J. Laane, J.R. Ohlsen, Characterization of nitrogen oxides by vibrational spectroscopy, Prog. Inorg. Chem. 87 (1980) 465–509.
[32] F. Paulat, T. Kuschel, C. Nather, V.K.K. Praneeth, O. Sander, N. Lehnert, Spectroscopic properties and electronic structure of pentammineruthenium(II) dinitrogen oxide and corresponding nitrosyl complexes: binding mode of N_2O and reactivity, Inorg. Chem. 43 (2004) 6979–6994.
[33] M. Hang, V. Huynh, R.T. Baker, D.L. Jameson, A. Labouriau, T.J. Meyer, Formation and reactivity of the Os(IV)-azidoimido complex, PPN[Os^{IV}(bpy)$(Cl)_3(N_4)$], J. Am. Chem. Soc. 124 (2002) 4580–4582.
[34] W.G. Lawrence, V.A.L. Apkarian, Infrared studies in free standing crystals: N_2O-doped Xe and Ar, J. Chem. Phys. 97 (1992) 2224–2228.
[35] G. Hussain, M.M. Rhaman, An infrared study of co-adsorption of N_2O and CO on ZnO, Spectrochim. Acta A 64 (2006) 880–885.